Available online at www.sciencedirect.com
ScienceDirect
Inorganica Chimica Acta 361 (2008) 1811–1818
Inorganica Chimica Acta
www.elsevier.com/locate/ica

N-Substituted indole-3-thiolate [4Fe–4S] clusters with a unique and tunable combination of spectral and redox properties

Erwin P.L. van der Geer [a], Qian Li [a], Gerard van Koten [a], Robertus J.M. Klein Gebbink [a,*], Bart Hessen [a,b]

[a] *Chemical Biology and Organic Chemistry, Faculty of Science, Universiteit Utrecht, Padualaan 8, 3584 CH Utrecht, The Netherlands*
[b] *Stratingh Institute, University of Groningen, Nijenborgh 4, 9747 AG Groningen, The Netherlands*

Received 10 September 2007; accepted 17 September 2007
Available online 22 September 2007

Abstract

A series of N-substituted indole-3-thiols, synthesized by sequential alkylation, thiouronium salt formation, and hydrolysis, are used to generate a novel family of [4Fe–4S] clusters. The redox transitions of the clusters deviate from those of other [4Fe–4S] cluster families, with half-wave potentials lying in a range midway between those of [4Fe–4S] clusters bound by aliphatic thiolate ligands and those bound by thiophenolate-based ligands. In UV–vis spectroscopy, the new cluster family shows absorption maxima that are among the most red-shifted reported thus far in [4Fe–4S] cluster chemistry. The indole-3-thiolate ligand thus leads to a highly specific and uncommon combination of [4Fe–4S] cluster properties, which can be fine-tuned by facile derivatization at the indole nitrogen atom.

Keywords: Iron; Sulfur; Cluster compounds; Indole-3-thiols; Substituent effects

1. Introduction

The cuboidal [4Fe–4S] cluster is one of the most abundant and ancient protein cofactors found in nature. Endowed with a rich redox chemistry, [4Fe–4S] clusters serve vital biological roles, including electron transport, sensing, and catalysis [1,2]. In conjunction with its importance in living systems, the synthetic accessibility of the [4Fe–4S] cluster has resulted in it being the focus of intense research since the beginning of biomimetic chemistry in the 1970s. Since then, a myriad of synthetic analogs has been prepared and analyzed, most of them in the 2− state [3].

Some of the most interesting results in the field have been obtained utilizing tripodal ligands preorganized to chelate three of the four iron atoms in the [4Fe–4S] cluster, leaving one iron atom free to undergo site-specific substitution chemistry [4]. The first such ligand to be reported was $L(SH)_3$ (Chart 1), prepared by Holm and co-workers, and numerous 3:1 site-differentiated cluster compounds with $L(SH)_3$ have since been prepared [3–5]. However, the difficult synthesis of $L(SH)_3$ has prevented its widespread use in biomimetics and several alternatives to $L(SH)_3$ have been reported. Of these alternatives, the $TriSH_3$ ligand (Chart 1), reported by Pohl and co-workers in 1997, is arguably the most promising [6]. Not only is $TriSH_3$ the only alternative to $L(SH)_3$ for which 1:1 reaction stoichiometry with [4Fe–4S] clusters has been proven crystallographically, [6] but our recent optimization of the synthesis of $TriSH_3$ has also rendered its preparation both convenient and high-yielding [7].

The synthetic accessibility of $TriSH_3$ is based in part on the versatility of indole. Indole cannot only be easily substituted at the nitrogen atom, but can also undergo regioselective electrophilic aromatic substitutions on the third position of the five-membered ring [8]. Taking advantage of this property, Harris has reported the synthesis of

* Corresponding author. Tel.: +31 30 2531889; fax: +31 30 2523615.
E-mail address: r.j.m.kleingebbink@uu.nl (R.J.M. Klein Gebbink).

0020-1693/$ - see front matter © 2007 Elsevier B.V. All rights reserved.
doi:10.1016/j.ica.2007.09.021

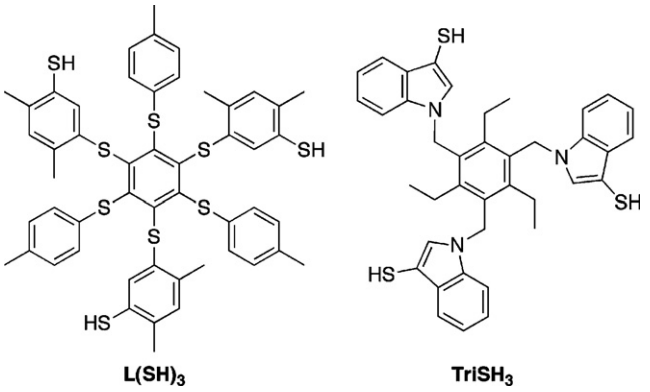

Chart 1. The tripodal ligands $L(SH)_3$ and $TriSH_3$.

indole-3-thiouronium iodide using thiourea and KI_3 as oxidant. The thiouronium salt was subsequently hydrolyzed to indole-3-thiol, a thiol that is aromatic but not nearly as acidic as thiophenol [9]. Indole-3-thiol can then be further derivatized to form $TriSH_3$ [6,7].

Despite the obvious relation of $TriSH_3$ to monodentate indole-3-thiols, [4Fe–4S] clusters fully coordinated by indole-3-thiolate ligands have yet to be reported. Nevertheless, the combination of ligand aromaticity and high electron-donating ability may lead to interesting, novel properties, while N-substitution allows for facile derivatization. In this paper, we report the use of sequential N-substitution and thiouronium salt formation to synthesize new, N-substituted indole-3-thiols, and the application of these thiols to generate an indole-3-thiolate-based family of [4Fe–4S] clusters.

2. Experimental

2.1. General

Reactants were purchased from Acros and used as received. All thiols and [4Fe–4S] clusters were handled under dry N_2 atmospheres using standard Schlenk or glovebox techniques. DMF and CH_2Cl_2 were distilled over CaH_2, while diethyl ether was distilled over Na/benzophenone. The ^1H NMR spectrum in Fig. 2 was recorded at 298 K on a Varian spectrometer operating at 400 MHz. All other ^1H and ^{13}C NMR spectra were recorded at 300 K on a Bruker AC 300 spectrometer operating at 300 and 75 MHz, respectively. The spectra were calibrated on the residual solvent peaks and spectral assignments were based on chemical shift, integral, and linewidth considerations. Contact shifts were calculated vs. ^1H NMR shifts of the free thiols in DMSO-d_6; however, since the thiols slowly oxidized in this solvent, full spectral characterizations of the thiols were carried out in $CDCl_3$ instead. Infrared spectra were recorded on a Perkin–Elmer Spectrum One FT-IR spectrometer. UV–vis spectra were recorded on a Varian Cary 50 Scan UV–vis spectrophotometer. Elemental analyses were carried out by Kolbe Mikroanalytisches Laboratorium (Mülheim an der Ruhr, Germany). Cyclic voltammograms were recorded at 100 mV/s using Pt working and counter electrodes, a Ag/AgCl reference electrode, and 0.1 M n-Bu_4NClO_4 in CH_2Cl_2 or MeCN as supporting electrolyte. Potentials were referenced to a ferrocene (Fc) internal standard. Fc was added directly to samples of all clusters except **3d**. Here, the Fc/Fc^+ wave was found to overlap with irreversible, multi-electron oxidation waves, and a separate blank run with Fc was run. Potentials vs. a standard calomel electrode (SCE) were calculated by taking $E_{1/2}$ $(Fc/Fc^+) = 0.424$ V vs. SCE in CH_2Cl_2 [10] and 0.379 V in MeCN [11].

2.2. 1-Methylindole-3-thiouronium iodide (*1b*)

A solution of thiourea (0.581 g, 7.63 mmol), I_2 (1.94 g, 7.63 mmol), and KI (1.27 g, 7.63 mmol) in a 4/1 (v/v) mixture of MeOH and H_2O (30 mL) was added to 1-methylindole (1.00 g, 7.63 mmol) and stirred overnight. The solution was concentrated *in vacuo* to yield an orange, crystalline material, which was collected by filtration, washed with water and ether, and dried *in vacuo*. Yield: 2.08 g (6.24 mmol, 82%). *Anal.* Calc. for $C_{10}H_{12}IN_3S$: C, 36.05; H, 3.63; N, 12.61; S, 9.62. Found: C, 36.09; H, 3.58; N, 12.53; S, 9.72%. ^1H NMR (DMSO-d_6): $\delta = 8.87$ (br s, 2H, NH_2), 8.55 (br s, 2H, NH_2), 7.97 (s, 1H, indolyl H2), 7.64 (d, $^3J_{H-H} = 8.3$ Hz, 1H, indolyl H), 7.51 (d, $^3J_{H-H} = 7.4$ Hz, 1H, indolyl H), 7.34 (t, $^3J_{H-H} = 7.6$ Hz, 1H, indolyl H), 7.25 (t, $^3J_{H-H} = 7.4$ Hz, 1H, indolyl H), 3.88 (s, 3H, CH_3). $^{13}C\{^1H\}$ NMR (DMSO-d_6): $\delta = 170.71$ ($C(NH_2)_2$), 139.43, 137.52, 128.72, 122.74, 121.24, 117.71, 111.16, 88.67 (8 × indolyl C), 33.27 (CH_3). FT-IR (ATR, ν, cm^{-1}): 3289, 3252, 3162, 3088, 1637, 1608, 1508, 1458, 1424, 1374, 1337, 1242, 1155, 1127, 1042, 840, 766, 745, 684.

1-Pentylindole-3-thiouronium iodide (**1c**), 1-decylindole-3-thiouronium iodide (**1d**), and 1-benzylindole-3-thiouronium iodide (**1e**) were synthesized analogous to **1b**. Full experimental details and characterizations are included as Supplementary material.

2.3. 1-Methylindole-3-thiol (*2b*)

A suspension of **1b** (2.082 g, 6.25 mmol) in aqueous NaOH (1 M, 25 mL) was heated to 90 °C for 10 min. After cooling to ambient temperature, aqueous HCl (2 M, 12.5 mL) was added, and the solution extracted with ether (3 × 15 mL). The ether was evaporated *in vacuo* and the residue was distilled to yield a colorless oil. Yield: 0.782 g (4.79 mmol, 77%). *Anal.* Calc. for C_9H_9NS: C, 66.22; H, 5.56; N, 8.58; S, 19.64. Found: C, 66.08; H, 5.51; N, 8.52; S, 19.70%. ^1H NMR ($CDCl_3$): $\delta = 7.73$ (d, $^3J_{H-H} = 8.3$ Hz, 1H, indolyl H), 7.35–7.19 (m, 3H, indolyl H), 7.15 (s, 1H, indolyl H2), 3.77 (s, 3H, CH_3), 2.89 (s, 1H, SH). $^{13}C\{^1H\}$ NMR ($CDCl_3$): 137.21, 133.21, 130.66, 122.45, 120.11, 119.52, 109.58, 95.37 (8 × indolyl C), 33.05 (CH_3). FT-IR (ATR, ν, cm^{-1}): 3108, 3050, 2942,

2518, 1613, 1514, 1481, 1461, 1421, 1357, 1333, 1317, 1240, 1154, 1128, 1110, 1010, 926, 806, 735.

1-Pentylindole-3-thiol (**2c**), 1-decylindole-3-thiol (**2d**), and 1-benzylindole-3-thiol (**2e**) were prepared similarly. Full experimental details and characterizations are included as Supplementary material.

2.4. $(n\text{-}Bu_4N)_2[Fe_4S_4(S\text{-}3\text{-}C_8H_6N)_4]$ (**3a**)

To a mixture of $(n\text{-}Bu_4N)_2[Fe_4S_4(S\text{-}t\text{-}Bu)_4]$ [12] (0.100 g, 0.0838 mmol) and indole-3-thiol [7,9] (63 mg, 0.42 mmol) was added DMF (7 mL). The mixture was stirred overnight to yield a dark violet solution, which was concentrated *in vacuo*. Addition of ether (60 mL) led to the formation of a fine black precipitate, which was collected by centrifugation, washed with ether, and dried *in vacuo*. ^{1}H NMR revealed the presence of 1.0 equiv. DMF. Yield: 0.115 g (0.0765 mmol, 91%). The product was dried further under ultra-high vacuum before elemental analysis, but 0.2 equiv. DMF remained. *Anal.* Calc. for $C_{64}H_{96}Fe_4N_6S_8 \cdot 0.2C_3H_7NO$: C, 53.73; H, 6.80; N, 6.01; S, 17.76. Found: C, 53.71; H, 6.77; N, 5.95; S, 17.75%. ^{1}H NMR (DMSO-d_6): $\delta = 10.35$ (br s, 4H, NH), 7.89 (br s, 4H, indolyl H), 7.43 (d, $^3J_{H-H} = 7.6$ Hz, 4H, indolyl H), 7.07 (br t, $^3J_{H-H} = 6.4$ Hz, 4H, indolyl H), 6.81 (br s, 4H, indolyl H), 4.34 (very br s, 4H, indolyl H2), 3.16 (t, $^3J_{H-H} = 8.4$ Hz, 16H, n-Bu_4N^+ α-CH_2), 1.56 (br quintet, $^3J_{H-H} = 7.7$ Hz, 16H, n-Bu_4N^+ β-CH_2), 1.30 (sextet, $^3J_{H-H} = 7.1$ Hz, 16H, n-Bu_4N^+ γ-CH_2), 0.93 (t, $^3J_{H-H} = 7.3$ Hz, 24 H, n-$Bu_4N^+CH_3$). λ_{max} (DMF, nm): 289, 303 (shoulder), 502. $E_{1/2}$ vs. Fc/Fc^+ in MeCN = −1.55 V ($\Delta E_p = 62$ mV) [2−/3−]. $E_{1/2}$ vs. SCE in MeCN = −1.17 V [2−/3−].

2.5. $(n\text{-}Bu_4N)_2[Fe_4S_4(S\text{-}3\text{-}C_8H_5N\text{-}1\text{-}CH_3)_4]$ (**3b**)

To a solution of $(n\text{-}Bu_4N)_2[Fe_4S_4(S\text{-}t\text{-}Bu)_4]$ [12] (0.129 g, 0.108 mmol) in DMF (5 mL) was added **2b** (0.088 g, 0.54 mmol). A periodic vacuum was applied to the stirred solution for 2 h, during which a color change from dark green to dark violet was observed. The solution was concentrated *in vacuo*. Addition of ether (40 mL) led to the formation of a fine black precipitate, which was collected by centrifugation, washed with ether, and dried *in vacuo*. Yield: 0.123 g (0.0828 mmol, 77%). *Anal.* Calc. for $C_{68}H_{104}Fe_4N_6S_8$: C, 54.98; H, 7.06; N, 5.66; S, 17.27. Found: C, 55.12; H, 7.02; N, 5.54; S, 17.20%. ^{1}H NMR (DMSO-d_6): $\delta = 8.00$ (br s, 4H, indolyl H), 7.45 (d, $^3J_{H-H} = 8.1$ Hz, 4H, indolyl H), 7.16 (br t, $^3J_{H-H} = 6.8$ Hz, 4H, indolyl H), 6.81 (br d, $^3J_{H-\ H} = 5.1$ Hz, 4H, indolyl H), 4.66 (very br s, 4H, indolyl H2), 4.45 (s, 12H, NCH_3), 3.15 (t, $^3J_{H-\ H} = 7.7$ Hz, 16H, n-Bu_4N^+ α-CH_2), 1.57 (br quintet, 16H, n-Bu_4N^+ β-CH_2), 1.31 (sextet, $^3J_{H-H} = 6.9$ Hz, 16H, n-Bu_4N^+ γ-CH_2), 0.93 (t, $^3J_{H-H} = 7.1$ Hz, 24H, n-Bu_4N^+ CH_3) λ_{max} (DMF, nm): 285, 304 (shoulder), 506. $E_{1/2}$ vs. Fc in MeCN = −1.54 V ($\Delta E_p = 98$ mV) [2−/3−]. $E_{1/2}$ vs. SCE in MeCN = −1.16 V [2−/3−]. $E_{1/2}$ vs. Fc/Fc^+ in CH_2Cl_2 = −1.59 V ($\Delta E_p = 75$ mV) [2−/3−], −0.53 V ($\Delta E_p = 68$ mV) [2−/1−]. $E_{1/2}$ vs. SCE in CH_2Cl_2 = −1.17 V [2−/3−], −0.10 V [2−/1−].

2.6. $(n\text{-}Bu_4N)_2[Fe_4S_4(S\text{-}3\text{-}C_8H_5N\text{-}1\text{-}C_5H_{11})_4]$ (**3c**)

A solution of $(n\text{-}Bu_4N)_2[Fe_4S_4(S\text{-}t\text{-}Bu)_4]$ [12] (0.0650 g, 0.0545 mmol) and **2c** (0.0538 g, 0.245 mmol) in DMF (5 mL) was stirred overnight, after which the DMF was removed *in vacuo*. The sticky black residue was dissolved in CH_2Cl_2 (10 mL) and filtered. Ether (60 mL) was added and a sticky, black product was collected by centrifugation, washed with ether, and dried under ultra-high vacuum. Yield: 0.0629 g (0.0368 mmol, 68%). *Anal.* Calc. for $C_{84}H_{136}Fe_4N_6S_8$: C, 59.00; H, 8.02; N, 4.91; S, 15.00. Found: C, 58.87; H, 7.91; N, 4.88; S, 14.96%. ^{1}H NMR (DMSO-d_6): $\delta = 7.98$ (br s, 4H, indolyl H), 7.48 (d, $^3J_{H-H} = 7.4$ Hz, 4H, indolyl H), 7.13 (br t, $^3J_{H-H} = 5.8$ Hz, 4H, indolyl H), 6.79 (br d, $^3J_{H-\ H} = 4.7$ Hz, 4H, indolyl H), 4.76 (very br s, 4H, indolyl H2), 4.56 (br s, 8H, pentyl α-CH_2), 3.16 (t, $^3J_{H-H} = 8.2$ Hz, 16H, n-Bu_4N^+ α-CH_2), 1.70 (s, 8H, pentyl β-CH_2), 1.54 (br quintet, $^3J_{H-H} = 7.7$ Hz, 16H, n-Bu_4N^+ β-CH_2), 1.31 (sextet, $^3J_{H-H} = 7.3$ Hz, 16H, n-Bu_4N^+ γ-CH_2), 1.23 (br s, 16H, pentyl CH_2), 0.93 (t, $^3J_{H-H} = 7.3$ Hz, 24H, n-Bu_4N^+ CH_3), 0.80 (br t, 12H, pentyl CH_3). λ_{max} (DMF, nm): 286, 305 (shoulder), 511. $E_{1/2}$ vs. Fc/Fc^+ in CH_2Cl_2 = −1.64 V (ΔE_p = 84 mV) [2−/3−], −0.56 V ($\Delta E_p = 72$ mV) [2−/1−]. $E_{1/2}$ vs. SCE in CH_2Cl_2 = −1.22 V [2−/3−], −0.14 V [2−/1−].

2.7. $(n\text{-}Bu_4N)_2[Fe_4S_4(S\text{-}3\text{-}C_8H_5N\text{-}1\text{-}C_{10}H_{21})_4]$ (**3d**)

To a solution of $(n\text{-}Bu_4N)_2[Fe_4S_4(S\text{-}t\text{-}Bu)_4]$ [12] (0.148 g, 0.124 mmol) in DMF (10 mL) was added **2d** (0.162 g, 0.560 mmol). A periodic vacuum was applied to the stirred solution for 4 h, during which a color change from dark green to dark violet was observed. After a further 16 h of stirring, the DMF was removed *in vacuo*. The resulting sticky black residue was dissolved in CH_2Cl_2 (10 mL) and filtered. The solution was then concentrated *in vacuo* to 5 mL, ether was added (60 mL), and the mixture kept at −20 °C for several hours. A fine black powder was collected by centrifugation, washed twice with ether, and dried *in vacuo*. ^{1}H NMR revealed the presence of 1 equiv. ether. Yield: 0.211 g (0.102 mmol, 82%). The ether was removed from the product under ultra-high vacuum prior to further analyses. *Anal.* Calc. for $C_{104}H_{176}Fe_4N_6S_8$: C, 62.76; H, 8.91; N, 4.22; S, 12.89. Found: C, 62.64; H, 8.97; N, 4.18; S, 12.76%. ^{1}H NMR (DMSO-d_6): $\delta = 7.96$ (br s, 4H, indolyl H), 7.48 (d, $^3J_{H-H} = 7.9$ Hz, 4H, indolyl H), 7.12 (br t, $^3J_{H-H} = 6.7$ Hz, 4H, indolyl H), 6.80 (br s, 4H, indolyl H), 4.80 (very br s, 4H, indolyl H2), 4.57 (br s, 8 H, decyl α-CH_2), 3.16 (t, $^3J_{H-H} = 8.3$ Hz, 16H, n-Bu_4N^+ α-CH_2), 1.70 (s, 8H, decyl β-CH_2), 1.54 (br t, $^3J_{H-H} = 7.7$ Hz, 16H, n-Bu_4N^+ β-CH_2), 1.31 (sextet, $^3J_{H-H} = 7.3$ Hz, 16H, n-Bu_4N^+ γ-CH_2), 1.19 (br s, 56H, decyl CH_2), 0.93 (t, $^3J_{H-H} = 7.4$ Hz, 24H, n-Bu_4N^+ CH_3), 0.83 (t, $^3J_{H-H}$ =

6.5 Hz, 12H, decyl CH_3). λ_{max} (DMF, nm): 287, 305 (shoulder), 510. $E_{1/2}$ vs. Fc/Fc^+ in $CH_2Cl_2 = -1.63$ V ($\Delta E_p =$ 110 mV) [2−/3−], −0.56 V ($\Delta E_p = 72$ mV) [2−/1−]. $E_{1/2}$ vs. SCE in $CH_2Cl_2 = -1.20$ V [2−/3−], −0.14 V [2−/1−].

2.8. $(n\text{-}Bu_4N)_2[Fe_4S_4(S\text{-}3\text{-}C_8H_5N\text{-}1\text{-}Bn)_4]$ (3e)

To a solution of $(n\text{-}Bu_4N)_2[Fe_4S_4(S\text{-}t\text{-}Bu)_4]$ [12] (0.161 g, 0.135 mmol) in DMF (10 mL) was added **2e** (0.162 g, 0.677 mmol). A periodic vacuum was applied to the stirred solution for 5 h, during which a color change from dark green to dark violet was observed. The solution was concentrated *in vacuo*. Addition of ether (40 mL) led to the formation of a fine black precipitate, which was collected by centrifugation, washed with ether, and dried *in vacuo*. Yield: 0.242 g (0.135 mmol, quant.). *Anal.* Calc. for $C_{92}H_{120}Fe_4N_6S_8$: C, 61.74; H, 6.76; N, 4.70; S, 14.33. Found: C, 61.82; H, 6.73; N, 4.59; S, 14.37%. ^{1}H NMR (DMSO-d_6): $\delta = 7.98$ (br s, 4H, indolyl H), 7.45 (d, $^3J_{H-H} = 7.9$ Hz, 4H, indolyl H), 7.36–7.00 (m, 24H, indolyl and phenyl H), 6.80 (br s, 4H, indolyl H), 5.66 (br s, 8H, NCH_2), 5.03 (very br s, 4H, indolyl H2) 3.16 (t, $^3J_{H-H} =$ 7.9 Hz, 16H, n-Bu_4N^+ α-CH_2), 1.56 (br quintet, 16H, n-Bu_4N^+ β-CH_2), 1.30 (sextet, $^3J_{H-H} = 7.1$ Hz, 16H, n-Bu_4N^+ γ-CH_2), 0.93 (t, $^3J_{H-H} = 7.4$ Hz, 24H, n-Bu_4N^+ CH_3). λ_{max} (DMF, nm): 285 (shoulder), 305 (shoulder), 500. $E_{1/2}$ vs. Fc/Fc^+ in $CH_2Cl_2 = -1.60$ V ($\Delta E_p = 107$ mV) [2−/3−], −0.54 V ($\Delta E_p = 65$ mV) [2−/1−]. $E_{1/2}$ vs. SCE in $CH_2Cl_2 = -1.18$ V [2−/3−], −0.12 V [2−/1−].

3. Results and discussion

3.1. Synthesis of N-substituted indole-3-thiols 2a–e and [4Fe–4S] clusters 3a–e

In order to test the general applicability of our synthetic approach to [4Fe–4S] clusters with alkyl- and aryl-substituted indole-3-thiolate ligands, we synthesized a series of five indole-3-thiols with varying N-substituents (Scheme 1). Unsubstituted indole-3-thiol **2a** [7,9] and its methyl- [13] and benzyl-substituted [6] analogs **2b** and **2e** have been prepared previously by Harris's method, although synthetic details for **2b** and **2e** were not reported. Two alkyl-substituted indole-3-thiols with longer aliphatic substituents (**2c** = pentyl, **2d** = decyl) were prepared analogously from the known compounds 1-pentylindole [14] and 1-decylindole [15]. The two-step yields of thiols **2b–e** ranged from 40% to 63%.

Indole-3-thiols **2a–e** were then used to generate the five new [4Fe–4S] clusters **3a–e** by means of thiol exchange reactions [16,17] in DMF (Scheme 1). In each case, the formation of a deep violet color accompanied product formation. After reaction, the clusters **3a–e** could be isolated easily by means of precipitation from DMF or CH_2Cl_2, with elemental analyses confirming the high purity of the products.

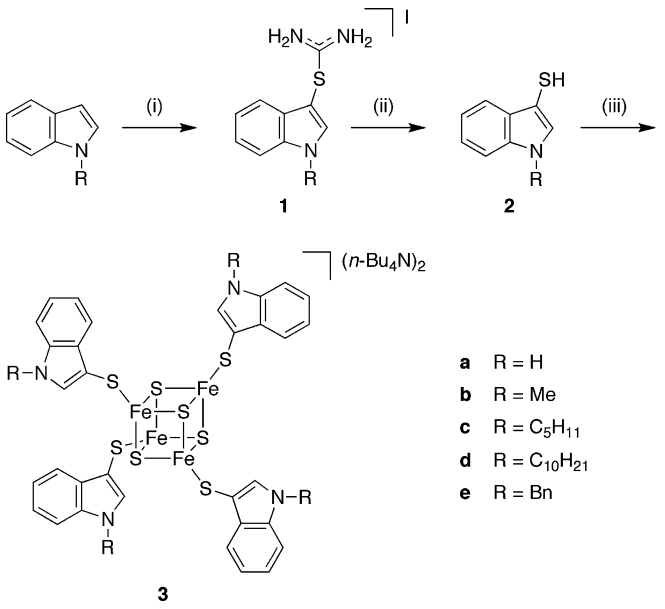

Scheme 1. Synthesis of clusters **3a–e**. Conditions: (i) thiourea/KI_3 in $MeOH/H_2O$. (ii) 1. $NaOH_{(aq)}$; 2. $HCl_{(aq)}$. (iii) $(n\text{-}Bu_4N)_2[Fe_4S_4(S\text{-}t\text{-}Bu)_4]$ in DMF, vacuum.

The physical–chemical effects of N-substitution are clearly manifest in the differential solubilities of clusters **3a–e**. While unsubstituted cluster **3a** is insoluble in CH_2Cl_2, solubility is good for clusters **3b–e**, and **3d** even shows appreciable solubility in 10:1 mixtures of ether and CH_2Cl_2. Compounds **3b–e** further show good solubility in MeCN, THF, DMSO, and DMF. The decyl chains give **3d** a greasy texture, in line with the amphiphilic properties of 1-decylindole reported by Abel et al. [15]. Variation of the N-substituent in this new [4Fe–4S] cluster family thus allows effective tuning of cluster lipophilicity.

3.2. ^{1}H NMR analysis

The ^{1}H NMR spectra of clusters **3a–e** show the characteristic contact shifting expected for ligands bound to a [4Fe–4S] cluster (Fig. 1, Table 1) [18].

Throughout the series of clusters, the contact shifting is greatest for the indolyl H2 nucleus. This proton is bound to the ring at a position which receives delocalized positive spin density from the cluster-bound sulfur atom, and it is also the hydrogen atom closest to the cluster. Interestingly, a ^{1}H NMR signal was never observed for the analogous H2 protons of $TriSH_3$ after coordination to [4Fe–4S] clusters [6,7].

Within the group of clusters **3a–e**, the magnitude of the H2 contact shift is highest in non-alkylated cluster **3a**. N-Methylation decreases the contact shift by more than 0.3 ppm, while extension of the alkyl chain through the pentyl to the decyl group leads to a further decrease of almost 0.1 ppm. This indicates that electron-releasing substituents on the indole nitrogen atom have a significant effect on the spin density at the H2 atom. The strongest H2 contact shift attenuation, however, is observed upon

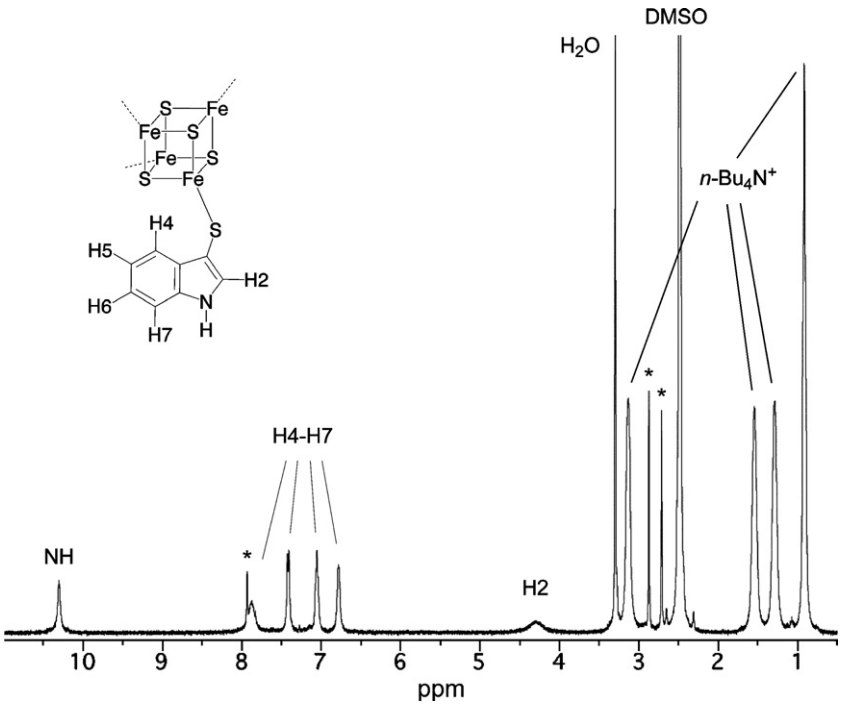

Fig. 1. ^{1}H NMR spectrum of **3a** in DMSO-d_6. DMF signals are marked with asterisks.

Table 1
Contact shifts (vs. free ligands) of selected hydrogen atoms in **3a**–**e**

Compound	R	Contact shift, ppm		
		H2	NH	α-H
3a	H	−3.09	−0.89	n/a
3b	Me	−2.77	n/a	0.70
3c	C_5H_{11}	−2.72	n/a	0.43
3d	$C_{10}H_{21}$	−2.68	n/a	0.44
3e	Bn	−2.60	n/a	0.26

substitution with a benzyl group. The reason for this effect is unclear, but may be related to a difference in shielding of the H2 atom caused by the orientation of the benzyl group upon coordination of **2e** to a [4Fe–4S] cluster.

For the unsubstituted cluster **3a**, the contact shift of the NH proton is also negative, albeit significantly less negative than that of the H2 proton. The fact that both the NH and H2 protons are shifted to lower frequencies by contact interactions indicates the presence of same-sign spin densities at positions 1 and 2 of the indole-3-thiolate ligand. An analogous spin distribution has been found in the indole radical cation, [19] in contrast to thiophenolate-based systems, in which neighboring hydrogen atoms generally display opposite-sign contact shifts [18].

While the NH protons in **3a** display a negative contact shift, the shifts of the indole substituent α protons in **3b**–**e** are all positive. This observation parallels the results obtained by Holm and co-workers, who also observed opposite-sign contact shifts for the *para* hydrogen atom in $[Fe_4S_4(SPh)_4]^{2-}$ and the methyl protons in its *p*-tolyl analog, $[Fe_4S_4(SC_6H_4\text{-}p\text{-}Me)_4]^{2-}$ [18]. Meanwhile, the magnitudes of the α proton contact shifts follow a similar trend as that observed for the H2 protons. The methyl protons show a positive shift of 0.70 ppm, which is significantly larger than for the pentyl and decyl α methylene signals. Again, the smallest contact shift is observed for the benzyl substituent.

3.3. Cyclic voltammetry

The electrochemical properties of **3b**–**e** were studied by cyclic voltammetry in CH_2Cl_2 while, due to its insolubility in this solvent, **3a** was studied in MeCN. For comparison, a cyclic voltammogram in MeCN was also obtained for **3b** (Table 2).

Each of the clusters **3b**–**e** undergoes a chemically reversible 2−/3− transition in CH_2Cl_2 solution (Fig. 2). The peak currents vary linearly with the square root of the scan rate, as expected for an electrochemically reversible process.

Table 2
Electrochemical data for **3a**–**e** (vs. SCE, 100 mV/s)

Compound	R	Solvent	$E_{1/2}$ [2−/3−] (V)	ΔE_p (mV)	$E_{1/2}$ [2−/1−] (V)	ΔE_p (mV)
3a	H	MeCN	−1.17	62	Irreversible	n/a
3b	Me	MeCN	−1.16	98	Irreversible	n/a
3b	Me	CH_2Cl_2	−1.17	75	−0.10	68
3c	C_5H_{11}	CH_2Cl_2	−1.22	84	−0.14	72
3d	$C_{10}H_{21}$	CH_2Cl_2	−1.20	110	−0.14	72
3e	Bn	CH_2Cl_2	−1.18	107	−0.12	65

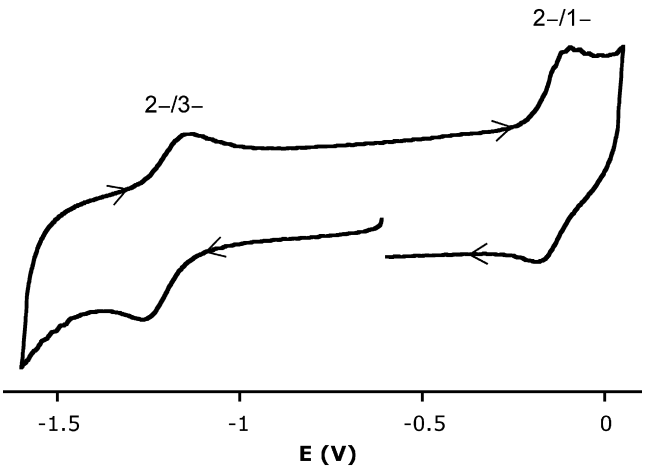

Fig. 2. Cyclic voltammogram of **3d** in CH_2Cl_2 (vs. SCE, 100 mV/s).

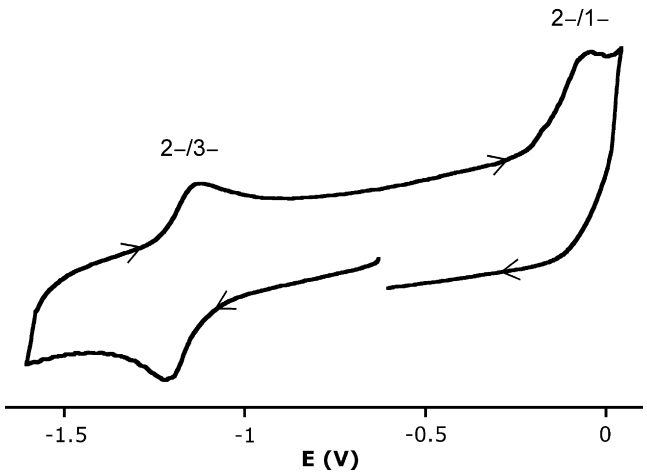

Fig. 3. Cyclic voltammogram of **3a** in MeCN (vs. SCE, 100 mV/s).

However, the peak separations exceed the theoretical value of 59 mV and increase with the scan rate, implying that the 2−/3− transition is quasi-reversible.

The 2−/1− transitions, on the other hand, are not chemically reversible. Similar to the related, TriS-chelated [4Fe–4S] clusters, [7] the oxidation waves for these transitions are significantly more intense than the corresponding reduction waves, implying that the 1− state decomposes on the time scale of the cyclic voltammetry experiment. The asymmetry between the waves can be reduced by increasing the scan rate, thereby limiting the extent of decomposition.

From the redox potentials in Table 2, it is evident that the N-substituent has a subtle but observable effect on the electrochemical properties of **3b–e**. Reduction of the pentyl- and decyl-substituted clusters **3c** and **3d** requires potentials of −1.22 and −1.20 V vs. SCE, respectively. Benzylated cluster **3e** displays the 2−/3− redox process at the slightly less negative potential of −1.18 V, while methylated cluster **3b** is the most easily reduced cluster of the series ($E_{1/2} = -1.17$ V). A similar trend is exhibited by the 2−/1− transition.

For [4Fe–4S] clusters coordinated by *para*-substituted thiophenolates, the redox potential displays a linear dependence on the Hammett σ_p values [20]. The effect of the N-substituent on the redox potential of **3b–e**, however, appears to be less straightforward. This is clearly exemplified by decyl-substituted compound **3d**, which displays a slightly less negative 2−/3− redox potential than **3c** despite its longer alkyl chain.

The electrochemistry of cluster **3a**, which is insoluble in CH_2Cl_2, was studied in MeCN. The cyclic voltammogram only shows reversibility for the 2−/3− process, with the 1− state apparently unstable in the presence of potentially nucleophilic solvent molecules (Fig. 3). The observed peak separation for the 2−/3− redox process is close to the theoretical minimum of 5 mV, but increases with increasing scan speed, implying quasi-reversibility. Again, a linear relationship exists between the peak potentials and the square root of the scan speed.

In MeCN, methyl-substituted cluster **3b** shows similar cyclic voltammetry behavior to **3a**, despite the electron-donating ability of the methyl group. A possible explanation for this result is the fact that the NH groups in **3a** can hydrogen-bond to electron-rich solvent molecules, thereby parallelling the effects of methylation. Intramolecular N–H–S hydrogen bonds are known to lead to positive redox potential shifts in CH_2Cl_2 [21–23]. The rigidity of the indole-3-thiolate ligand prevents such intramolecular hydrogen bonding in **3a**, leaving the NH groups free to hydrogen bond with MeCN.

In general, all the redox potentials in Table 2 are more negative than the potentials found for symmetrically substituted, thiophenolate-bound [4Fe–4S] clusters in MeCN and CH_2Cl_2, but more positive than those observed in clusters with alkylthiolate ligands [20,24]. In fact, it appears that the redox processes of indole-3-thiolate [4Fe–4S] clusters occur in an intermediate potential range deviating from the redox potentials of all other symmetrically substituted [4Fe–4S] clusters, thereby reflecting the intermediate electron-donating strength of indole-3-thiolate ligands. The closest redox potential that we could find in literature for a symmetrically substituted [4Fe–4S] cluster is that of $(Me_4N)_2[Fe_4S_4(SC_6H_4\text{-}p\text{-}NMe_2)_4]$, reported by Holm and co-workers [20]. The highly electron-donating dimethylamino substituent in this cluster shifts the redox potential to approximately −1.1 V, which, however, is still substantially less negative than the redox potential of **3a** [20].

On the other hand, the 3:1 site-differentiated cluster $(n\text{-}Bu_4N)_2[Fe_4S_4(TriS)(SC_6H_4\text{-}p\text{-}F)]$ (**4**) displays a 2−/3− redox potential of −1.19 V, close to the potentials of the related clusters **3b–e** [7]. Cluster **4** is a mixed-ligand system, with one *p*-fluorothiophenolate ligand and three indole-3-thiolate binding moieties belonging to the TriS ligand. Johnson and Holm have demonstrated that in such mixed-ligand clusters, the redox properties are determined by the sum of the four, independent ligand contributions [25]. Given that the redox potential of $(n\text{-}Bu_4N)_2$

$[Fe_4S_4(SC_6H_4\text{-}p\text{-}F)_4]$ (**5**) is −1.01 V [7] the contribution of each indole-3-thiolate arm to the redox potential of **4** is then $((-1.19 - (0.25 \times -1.01))/3)$ V = −0.3125 V. An imaginary cluster chelated by four of such arms would thus have a redox potential of −1.25 V, more negative than the potentials observed for **3b**–**e**. Hence, the TriS ligand appears to induce more negative redox potential shifts than non-chelating analogs. This effect possibly stems from the π electron cloud of the TriS ligand's central aryl ring, which is forced to assume a position close to the cluster core upon chelation.

The redox potentials for the 2−/1− processes in **4** and **5**, meanwhile, are −0.06 and +0.10 V, respectively [7]. Using the same reasoning as above, the contribution of each TriS indole-3-thiolate arm to the 2−/1− redox potential is then $((-0.06 - (0.25 \times\ 0.10))/3)$ V = −0.028 V. A cluster chelated by four such arms would display a 2−/1− redox transition at a potential of −0.11 V, which falls in the same range as the redox potentials exhibited by **3b**–**e**. Hence, for the 2−/1− redox process, the TriS ligand appears to behave more as the sum of three indole-3-thiolates.

3.4. UV–vis spectroscopy

Compounds **3a**–**e** are all intensely violet in DMF solution, and display several electronic transitions (Fig. 4 and Table 3).

All five new cluster compounds show intense absorptions between 285 and 289 nm (maxima for all clusters except **3e**) and around 304 nm (shoulders). Local maxima are also observed between 500 and 511 nm, while additional weak features are present between 370 and 450 nm.

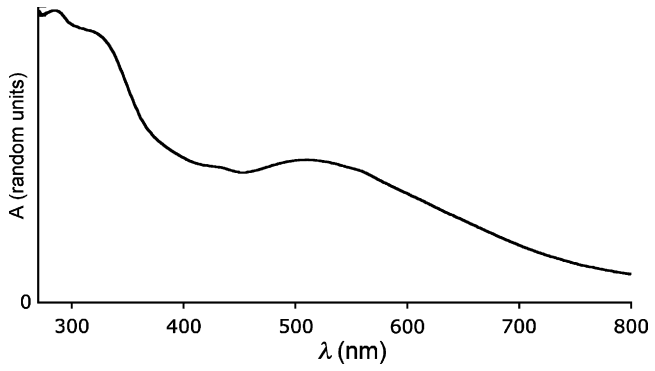

Fig. 4. UV–vis spectrum of **3c** in DMF.

Table 3
Principal UV–vis absorptions of **3a**–**3e** in DMF

Compound	R	$\lambda_{max,1}$ (nm)	$\lambda_{max,2}$ (nm)	$\lambda_{max,3}$ (nm)
3a	H	289	303[a]	502
3b	Me	285	304[a]	506
3c	C_5H_{11}	286	305[a]	511
3d	$C_{10}H_{21}$	287	305[a]	510
3e	Bn	285[a]	305[a]	500

[a] Shoulder.

Transitions between 280 and 300 nm in [4Fe–4S] clusters have been assigned to charge-transfer processes from inorganic sulfide to iron 3d orbitals [26]. The energies of the corresponding transitions in the series **3a**–**e** lie in between those generally found for clusters with purely aliphatic (297 nm and higher) and those with aromatic thiolate ligands (275 nm and lower), and are similar to that in $[Fe_4S_4(SBn)_4]^{2-}$ (approximately 286 nm) [20]. Within the series **3a**–**e**, this transition appears little affected by the indole N-substituent. On the other hand, N-substitution does to some extent affect the maxima lying between 500 and 511 nm, with significant redshifts observed upon substitution with a methyl group or with the longer pentyl and decyl chains. Benzyl-substituted cluster **3e** again behaves differently from the other clusters, displaying the least redshifted absorption. Nonetheless, even the 500 nm transition in **3e** is among the most redshifted known in [4Fe–4S] cluster chemistry. To our knowledge, **3c** even displays the most redshifted maximum in DMF solutions reported so far, approached only by the cluster $(Me_4N)_2[Fe_4S_4(SC_6H_4\text{-}p\text{-}NMe_2)_4]$ mentioned earlier (510 nm) [20]. Although the exact origin of this electronic transition remains unclear, the parallel found between this cluster and **3a**–**e** suggests that the transition is most strongly redshifted by highly electron-donating, aromatic thiolates.

4. Conclusion

The thiolation of indole via electrophilic addition of bis(thiouronium)iodide and subsequent hydrolysis can be applied to a broad range of N-substituted indoles, providing convenient access to a relatively unexplored family of thiols and a corresponding family of indole-3-thiolate [4Fe–4S] clusters. The new cluster family displays several unique and distinguishing properties, including highly redshifted absorptions in the visible region and redox potentials that fall in a range deviating from all other groups of synthetic, symmetrically substituted [4Fe–4S] clusters. Their unique redox potentials make the indole-3-thiolate [4Fe–4S] clusters a valuable addition to the synthetic [4Fe–4S] clusters available for incorporation into catalysts or other functional (biomimetic) materials, in which the envisioned applications may impose strict requirements on the clusters' electrochemical properties.

Within the family of indole-3-thiolate clusters itself, facile derivatization is possible by means of substitution at the indole nitrogen atom. The current study shows that such substitution allows for fine-tuning of electrochemical, spectral, and physical properties, although the unexpected effects of N-benzylation indicate that the substituent effects may as yet prove difficult to predict. Apart from the fine-tuning of cluster properties, N-substituents may also prove useful as synthetic handles. Hence, we are currently exploring the synthesis of indole-3-thiolate [4Fe–4S] clusters with solid surface-binding domains, in order to study the effects of immobilizing [4Fe–4S] clusters onto well-defined interfaces.

Acknowledgement

This work was supported by the National Research School Combination–Catalysis (NRSC–C).

Appendix A. Supplementary material

Supplementary data associated with this article can be found, in the online version, at doi:10.1016/j.ica.2007.09.021.

References

[1] H. Beinert, R.H. Holm, E. Münck, Science 277 (1997) 653.
[2] M.K. Johnson, Curr. Opin. Chem. Biol. 2 (1998) 173.
[3] P. Venkateswara Rao, R.H. Holm, Chem. Rev. 104 (2004) 527.
[4] R.H. Holm, Pure Appl. Chem. 70 (1998) 931.
[5] T.D.P. Stack, R.H. Holm, J. Am. Chem. Soc. 109 (1987) 2546.
[6] C. Walsdorff, W. Saak, S. Pohl, J. Chem. Soc., Dalton Trans. (1997) 1857.
[7] E.P.L. van der Geer, G. van Koten, R.J.M. Klein Gebbink, B. Hessen, to be published.
[8] R.J. Sundberg, in: A.R. Katritzky, O. Meth-Cohn, C.S. Rees (Eds.), Indoles, Best Synthetic Methods, Academic Press Limited, London, The United Kingdom, 1996, p. 105.
[9] R.L.N. Harris, Tetrahedron Lett. (1969) 4465.
[10] M. Masui, H. Sayo, Y. Tsuda, J. Chem. Soc. B (1968) 973.
[11] I.M. Kolthoff, F.G. Thomas, J. Phys. Chem. 69 (1965) 3049.
[12] G.C. Christou, C.D. Garner, J. Chem. Soc., Dalton Trans. (1979) 1093.
[13] A.G. Schultz, W.Y. Fu, R.D. Lucci, B.G. Kurr, K.M. Lo, M. Boxer, J. Am. Chem. Soc. 100 (1978) 2140.
[14] A. Barco, S. Benetti, G.P. Pollini, P.G. Baraldi, Synthesis (1976) 124.
[15] E. Abel, M.F. Fedders, G.W. Gokel, J. Am. Chem. Soc. 117 (1995) 1265.
[16] M.A. Bobrik, L. Que Jr., R.H. Holm, J. Am. Chem. Soc. 96 (1974) 285.
[17] L. Que Jr., M.A. Bobrik, J.A. Ibers, R.H. Holm, J. Am. Chem. Soc. 96 (1974) 4168.
[18] R.H. Holm, W.D. Phillips, B.A. Averill, J.J. Mayerle, T. Herskovitz, J. Am. Chem. Soc. 96 (1974) 2109.
[19] S.E. Walden, R.A. Wheeler, J. Phys. Chem. 100 (1996) 1530.
[20] B.V. DePamphilis, B.A. Averill, T. Herskovitz, L. Que Jr., R.H. Holm, J. Am. Chem. Soc. 96 (1974) 4159.
[21] N. Ueyama, T. Terakawa, M. Nakata, A. Nakamura, J. Am. Chem. Soc. 105 (1983) 7098.
[22] N. Ueyama, A. Kajiwara, T. Terakawa, S. Ueno, A. Nakamura, Inorg. Chem. 24 (1985) 4700.
[23] R. Ohno, N. Ueyama, A. Nakamura, Inorg. Chem. 30 (1991) 4887.
[24] H.L. Blonk, O. Kievit, E.K.-H. Roth, J. Jordanov, J.G.M. van der Linden, J.J. Steggerda, Inorg. Chem. 30 (1991) 3231.
[25] R.W. Johnson, R.H. Holm, J. Am. Chem. Soc. 100 (1978) 5338.
[26] A. Aizman, D.A. Case, J. Am. Chem. Soc. 104 (1982) 3269.